

**VORTEX INDUCED VIBRATION (VIV) REDUCTION MEASURE ON
DIMPLED CONCRETE COATED PIPELINE**

SYAZWAN BIN SAZALI

**MECHANICAL ENGINEERING
UNIVERSITI TEKNOLOGI PETRONAS
JANUARY 2016**

**Vortex Induced Vibration (VIV) Reduction Measure on Dimpled
Concrete Coated Pipeline**

By

SYAZWAN BIN SAZALI

15988

**Dissertation report in partial fulfilment of the requirements for the
Bachelor of Engineering (Hons)
(Mechanical Engineering)**

FYP II JANUARY 2016

**Universiti Teknologi PETRONAS,
32610 Bandar Seri Iskandar,
Perak Darul Ridzuan**

CERTIFICATION OF APPROVAL

VIV Reduction Measure on Dimpled Concrete Coated Pipeline

By

Syazwan bin Sazali

15988

Dissertation submitted in partial fulfilment of
the requirements for the
Bachelor of Engineering (Hons.)
(Mechanical Engineering)

JANUARY 2016

Approved by:

Dr William Pao

Universiti Teknologi PETRONAS
Bandar Seri Iskandar
31750 Tronoh
Perak Darul Ridzuan

CERTIFICATION OF ORIGINALITY

This is to certify that I am responsible for the work submitted in this project, that the original work is my own except as specified in the references and acknowledgements, and that the original work contained herein have not been undertaken or done by unspecified sources or persons.

SYAZWAN SAZALI

ACKNOWLEDGEMENT

First and foremost, the author would like to direct his obligations to praise and thank The Almighty Allah, The Most Gracious and The Most Merciful for His guidance and blessings for giving an opportunity for the author to complete this Final Year Project as part of requirements for Bachelor of Engineering (Hons.) in Mechanical Engineering at Universiti Teknologi PETRONAS (UTP).

Deserving the author's highest gratitude is his family member who have been there supporting him throughout the study period. They have given the author moral support and the strength to endure any hardship he had encountered and definitely without them, the author would have never succeed on making through all the obstacles.

Hereby deserving of special appreciation is to the author's supervisor for this project, Dr William Pao for his continuous guidance and support provided throughout the progression of his project.

It is also my duty to record my thankfulness and giving credit to UTP specifically Mechanical Engineering Department which has always inspire their students and equipped them with essential skills for self-learning.

Last but not least, to all of the unsung heroes throughout the author's study program, his family, lecturers, friends, and colleagues, thank you very much for their patience, love and continuous support and absolutely without their advices and strength, the would not be able to complete his study and Final Year Project. The author salutes them all for their commitment to excellence in their field of expertise and send best wishes for a memorable journey waits ahead.

ABSTRACT

Pipelines due to high current and dynamic seabed topography, are exposed to free spanning and eventually leads to VIV formation. Effective VIV suppression devices are sought that will mitigate VIV and reduce drag for operation application. One of the ways to reduce the VIV is to adapt dimple onto the concrete coating of the marine pipeline. In this study, CFD analysis will be carried out for three cases which one of a regular pipeline, then for a pipeline attached with marine fairings and one with dimpled concrete coating pipeline. The motivation of doing such arrangement is to analyse the efficiency of the dimple geometry arrangement in order to suppress the vortex-induced vibration (VIV) of the corresponding marine pipeline.

In present work, the numerical simulation of flow past a circular cylinder, performed by using a commercial CFD code (ANSYS Fluent) with RANS ($k-\omega$ Shear-Stress Transport (SST) model) approaches. A range of Reynolds number were simulated from range of $Re = 1 \times 10^4$ to 2.5×10^6 for three different cases, the first (Case 1) is a bare cylinder, the second case (Case 2) is a cylinder attached with dimple with dimple depth of diameter ratio ($k/d = 3 \times 10^{-3}$), the third case (Case 3) is a cylinder attached with dimple with dimple depth to diameter ratio of ($k/d=4 \times 10^{-3}$). Main parameters analysed under the scope of VIV reduction are the drag coefficient, size of wake region, values of Reynolds's Number and the angle of separation.

Numerical simulations have shown that a significant delay in point of separation from $\theta = 80^\circ$ to 92° , resulting in a drag reduction at $Re = 1 \times 10^4$ to 4×10^5 . Furthermore, the variation of drag coefficient with Reynolds number from the base case being compared to Case 1 was nearly the same, so that we can conclude that this project having validated thoroughly by published work. Some previous studies strongly support the present mechanism of drag reduction by dimples. Finally, the present study suggests that for the application of dimple on a concrete layer coating of pipeline reduced drag at $Re=1 \times 10^4$ to 4×10^5 . It also suggests that the point of separation can be delayed up to $\theta = 92^\circ$ and producing a much smaller wake region and showing smaller eddies of vortices.

TABLE OF CONTENT

CHAPTER 1.0: INTRODUCTION

1.1 Background of Study	1
1.2 Problem Statement	2
1.3 Objectives	3
1.4 Scope of Study	3

CHAPTER 2.0: LITERATURE REVIEW

2.1 Marine Pipeline & Free-Span	4
2.2 Vortex Induced Vibration (VIV)	6
2.3 Flow Regime	7
2.4 Drag	4
2.5 VIV Suppression	6
2.6 Dimples	7

CHAPTER 3.0 METHODOLOGY

3.1 Project Methodology	9
3.2 CFD Methodology	10
3.2.1 Fluid Solution Domain	11
3.2.2 Modelling Geometries	11
3.2.3 Mesh Generation	11
3.2.4 Boundary Conditions	11
3.3 Gantt Chart and Key milestone	10

CHAPTER 4.0 RESULT AND DISCUSSION

4.1 Mesh Independency Study	16
4.2 Flow Visualization – Near Wall Region	19
4.3 Flow Visualization – Wake Region	19
4.4 Forces and Coefficient	26

CHAPTER 5 CONCLUSION AND RECOMMENDATION

5.1 Conclusion	29
5.2 Recommendation	29
REFERENCES	30
APPENDICES	

LIST OF FIGURES

Figure 2.1: Free Spanning Pipeline	2
Figure 2.2: How Free Span can harm pipeline	7
Figure 2.3: Mechanism of Vortex Shedding	9
Figure 2.4: VIV acts on Free Spanning Pipeline	12
Figure 2.5: Cylinder Wake Pattern vs Reynolds Number	13
Figure 3.1: Overall Project Methodology	13
Figure 3.2: CFD Methodology	15
Figure 3.3: Rectangular Shaped Fluid Solution Domain	16
Figure 3.4: Top View of Fluid Domain	17
Figure 3.5: Geometry of Dimple ($k/d = 3 \times 10^{-3}$)	17
Figure 3.6: Structured Grid Mesh	18
Figure 3.7: Inflation Layer around Cylinder	18
Figure 3.8: Zoom-in Inflation Layer Meshing around Cylinder	19
Figure 3.9: Zoom-in Inflation Layer Meshing around Cylinder	20
Figure 4.1: Graph of Drag Coefficient vs Number of Grid Element	21
Figure 4.2: Instantaneous Contour of the Velocity, $Re = 1 \times 10^5$ for Case 1	22
Figure 4.3: Instantaneous Contours of Velocity view at Separation Point, $\theta = 80^\circ$ for Case 1	23
Figure 4.4: Instantaneous contours of the velocity, $Re = 1 \times 10^5$ for Case 2	24
Figure 4.5: Instantaneous contours of velocity view at separation point, $\theta = 92^\circ$ for Case 2	25
Figure 4.6: Instantaneous contours of velocity view at separation point (a) $\theta = 76^\circ$ for Case 3; (b) $\theta = 70^\circ$ for Case 4	27

Figure 4.7: Instantaneous contours of vorticity (wake region) at $Re = 1 \times 10^5$,
for (a) Case 1; (b) Case 2. 27

Figure 4.8: Instantaneous velocity vectors for Case 2 at (a) $Re = 3 \times 10^5$;
(b) $Re = 4 \times 10^5$ 27

Figure 4.9: Variation of C_d with Reynolds number for smooth cylinder
and present result from Case 1 27

Figure 4.10: Graph of C_d vs Reynolds number for smooth cylinder
and present result from Case 1 and Case 2 27

LIST OF TABLE

Table 4.1: Summary of Main Parameter	2
Table 4.2: Summary results of Mesh Independency Study	7

CHAPTER 1: INTRODUCTION

1.1 Background of Study

Offshore pipelines are key equipment primarily used for transporting oil and gas over long distance point of extraction or production to the points of consumption. Being a medium of transportation for oil and gas product, pipelines are also used for other purposes as Bai (2001) states that the other roles of offshore pipeline are as:

- Export (transportation) pipelines;
- Flow line to transfer product from a platform to export line;
- Water injection or chemical injection flow line;
- Flow line to transfer product between platforms, subsea manifolds and satellite wells;
- Pipeline bundles;

A distinction is sometimes made between a flowline and a pipeline. Flowline is a pipe laid on the seabed which allows the transportation of multiphase product came from the wellhead to the host structure offshore within a particular development field or even onshore. Meanwhile a pipeline is a pipe carrying a single phase product of oil or gas also from subsea wellhead or manifolds to the host structure. Offshore pipeline are commonly laid on the seabed or below it inside a scour or trench which acts as a means of safeguarding the pipeline against any fishing gear or trawling activities.

Malaysia meteorology and oceanography overview indicates that sea waves in Malaysia are primarily driven by the Monsoons with the roughest whether arriving from the North-Northeast during the monsoon period.

As for information, Malaysia regional hub for oil and gas particularly Terengganu, Sabah and Sarawak are prone to experience a rough sea throughout the year which leads to high current and wave causes the seabed condition to be very dynamic. Due to that event, Malaysia water seabed surface are dynamically changing and this eventually lead to the formation of free span.

Free span is defined as the gap between the pipe and the seabed. Bakhtiary *et al* (2007) mentioned that free spanning for offshore pipeline often occurs because of the unevenness of seabed floor as well as local scouring due to turbulence by flow and instability and thus it endangers the safe of running pipeline. Hence, if dynamic loads occur, free spanning pipelines are at risk from damage due to either by bending from externally applied hydrodynamic loadings or self-weight loadings or by a long term fatigue damage experienced from cyclic loadings due to vortex induced vibration (VIV).

Owen & Bearman (2000) mentioned that vortex shedding is a challenging field of study in fluid dynamics and it continues to present problems to engineers and designers in a number of key industrial areas. Fluid flow past a pipeline generate vortices due to the shear present in the boundary layer. This vortex, with higher flow velocity are accompanied by lower pressure will draw the smaller vortex from the opposing side across the wake centreline. The opposite vortices from this smaller vortex serves as vortices supply of the larger vortex allowing it to converge downstream.

This process is repeated in the reverse sense which then leads to the alternating vortex shedding from the pipeline. The time-varying non uniform pressure distribution around the pipeline resulting from the vortex shedding which then causes structural vibrations in both inline and cross-flow direction. In this case, the vortex induced vibration (VIV) can affect the pipeline integrity.

As the environmental conditions are given and fixed, the only way to reduce the VIV is by using an efficient control technique or VIV suppression device adapted to the pipeline framework. Several control methods are already been proposed or implemented in order to reduce the drag forces or to regulate the vortex shedding around pipeline. One of the theory that could be used to suppressed vortex induced vibration (VIV) is using the mechanism of drag reduction by dimpled surface. Flow

control can be achieved by modifying the surface of the bluff body by adding roughness to its surface.

In order to modify the flow characteristic, surface roughness is used widely by reducing the drag. In golf ball industry, dimples have been accepted to be regular practise since 1930s, when research showed how they could increase lift and reduce drag. Meanwhile some years back, Russian scientists discovered that dimples might act as a useful tool for drag reduction. Their hypothesis are basically based on an experimental work that measure the turbulent flows over surface with a regular arrangement of shallow dimples leading to a significant decrease of the skin-fraction drag. Dimples induce a turbulent boundary layer, which has higher momentum than laminar boundary layer and thus delays separation which reduce drag significantly. In this case of study, the big theory of drag reduction on dimpled surface will be adapted on to an offshore pipeline as method to reduce vortex induced vibration (VIV).

1.2 Problem Statement

Pipelines due to high current and dynamic seabed topography, are expose to free spanning and eventually leads to VIV formation. Effective VIV suppression device are sought that will mitigate VIV and reduce drag for operation application. Therefore, investigating flow characteristic and VIV mechanism on dimpled concrete coating pipeline under free spanning condition as a VIV suppression device is necessary.

1.3 Objectives

This study aims to:

- a) To analyse the effect of adapting the dimpled shaped concrete coated pipeline on Vortex Induced Vibration under free-spanning condition through simulation using Computational Fluid Dynamics (CFD) method.
- b) To analyse the changes in drag coefficient of the flow around dimpled concrete coated pipeline.
- c) To analyse changes in angle of separation of the blunt body (pipeline) under range of Reynolds number using CFD method.

1.4 Scope of Study

The scope of work has been to study the physics of cases and apply ANSYS FLUENT to simulate the flow and investigate the effect of adapting dimpled shaped concrete coating onto a pipeline as a vortex induced vibration (VIV) suppression device. A two-dimensional CFD analysis has been carried out for a cylinder with Reynolds Number of $Re = 1 \times 10^4$ to 2.5×10^6 . The main goal was to run the simulations and compare the results to published studies. Several cases shall be taken into account as main parameter of study. The first (Case 1) is a bare cylinder, the second case (Case 2) is a cylinder attached with dimple with dimple depth of diameter ratio ($k/d = 3 \times 10^{-3}$), the third case (Case 3) is a cylinder attached with dimple with dimple depth to diameter ratio of ($k/d=4 \times 10^{-3}$) and of the cases are in the vicinity of a rigid wall subjected to Reynolds Number, $Re = 1 \times 10^4$ to 2.5×10^6 . Another key parameter analysed under the scope of VIV reduction are the drag coefficient, size of wake region, values of Reynold's Number and the angle of separation. Throughout this study, density, viscosity of fluid and wave impact are considered and shall be remain constant because this study only focus on VIV reduction measure.

CHAPTER 2: LITERATURE REVIEW

The main study of this research is mainly about modelling and simulating flow around a dimpled concrete coated pipeline as a solution for Vortex induced vibration (VIV) problems for free-spanning pipeline using Computational Fluid Dynamics (CFD) method. Production of oil and gas from offshore field has created many unique engineering challenges and one of such challenges involves the use of marine pipeline that are susceptible to large drag and vibrations when in the existence of sea current. Pipelines are subjected to experience drag and continuous strain due to current and waves that arouse vortexes to shed from the sides of the pipeline. Induced drag and vibration may lead to cyclic loading and potentially lead to the failure of pipeline structure.

The safety of the pipeline structure can be further improved if the flow around them are better understood. Scour may occur just underneath the pipeline due to current flow when it is placed on seabed. This may lead to formation of suspended spans of the pipelines where it is hanging just above seabed. It is very important to know what kind of changes that take place in the flow around the pipeline (Sumer and Frescoed, 1997)

Several numerical and experimental studies have been carried out to investigate the flow around pipeline in the subcritical flow regime that have Reynolds Number ranging from 300 to 3×10^5 . Ong et al (2008, 2010) performed a two-dimensional analysis using k – epsilon turbulence model. In this section, there are several literatures from different kind of source in order to ensure the precision assist in achieving the main objective for this study.

2.1 Marine Pipeline & Free-Span

Oil industry utilize many type of marine or offshore pipeline to tie-up the sea surface and the seafloor. These pipeline are essential lifelines to transfer resources of the

continental shelf offshore to other region. The main reasons for this is that pipeline consume less energy than other ways of transportation (Palmer and King, 2004). Free span or suspended span normally occur in subsea pipelines due to irregularity or unevenness of seabed bathymetry and also by scouring due to installation activity of non-buried pipeline. Due to current trend of world economic situation, budget constraints or harsh sea condition, most of the pipeline installation takes the methods of lowering the pipeline from the lay barge to the sea bottom without being buried. Therefore, Bakhtiary et al. (2007) and Mehdi et al. (2012) both agree that due to unevenness of seabed, the section of pipeline that are not in contact with the seabed may form free span. Currents flowing across the free spanning pipelines cause the shedding and formation of vortices around pipeline.

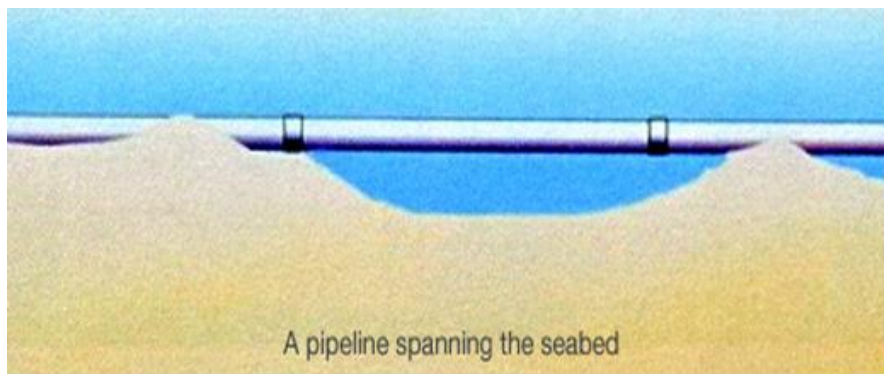


Figure 2.1: Free Spanning Pipeline

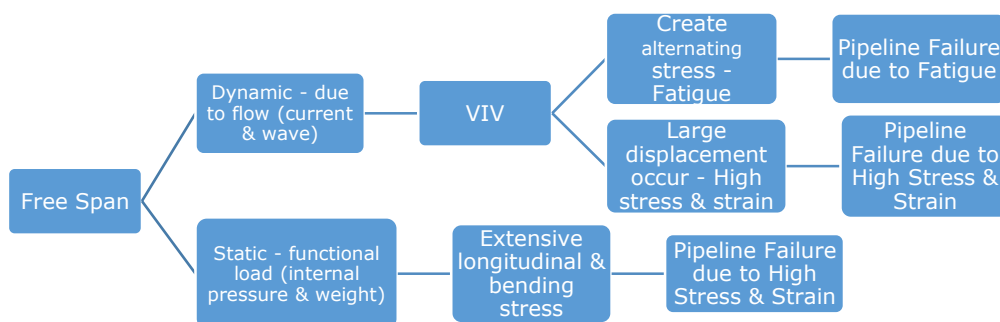


Figure 2.2: How Free Span can harm pipeline

2.3 Vortex Induced Vibration

In modern engineering practice, periodic shedding of vortices induced vibration are the most frequent case occur. The long span of marine pipeline on the seabed is prone to being exposed to the vortex induced vibrations imparted by the ocean current. Vortex induced vibrations (VIV) are a one of the example of instability induced vibrations. VIV occurs when there is an interaction of shedding frequencies of vortices generated by the ocean current flow around pipeline with one or more natural vibrations of the pipeline. This interaction results in high frequency stress reversal to the current flow which result in cyclic and large amplitude oscillations of the pipeline.

When a pipeline is placed in a flow, a shear layers of flow will be formed attributable to the separation of the boundary layer which occurs around the pipeline. The strength of the flow will increases and will further grows until a stronger shear layer breaks off the former shear layer as the shear layer moves away from the pipeline. Due to the pressure differences around the pipeline, vortices formed in the viscous boundary layer tend to detach at the downstream end of pipeline causing the pipeline to oscillate in the direction normal to the flow. The flow past the pipeline thus creates alternating low-pressure vortices on the downwind side of the pipeline. The pipeline will tend to move towards the low-pressure zone and then creates a cyclic like movement.

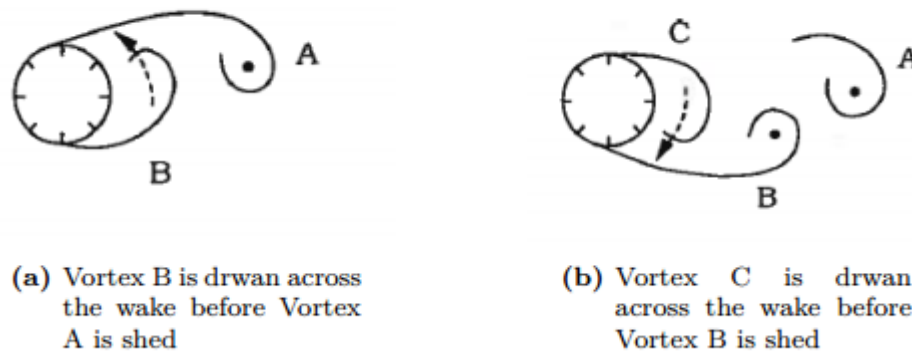


Figure 2.3: Mechanism of Vortex Shedding

Vortex shedding from pipeline is a challenging area. Large drag loads and possible vortex-induced vibration (VIV) of pipeline are important design issues in the current offshore industry. The shedding of the vortices causes a forced vibration to the pipeline which critically affects its remaining life. Subsea or marine pipeline system failure will be caused in a very short period of time due to severe fatigues damage implied on the pipeline while the vibration also significantly amplifies the global drag force of the pipeline system. Figure 2.4 shows a typical VIV of free spanning pipeline that illustrate flow and motion that acts on the pipeline.

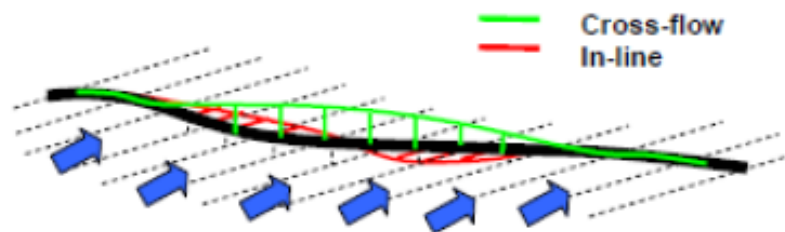


Figure 2.4: VIV acts on Free Spanning Pipeline

2.4 Flow Regime

The theory about flow regime stated by Sumer and Fredsoe (1997) is that a flow regime around a smooth circular cylinder in infinite fluid is described by the non-dimensional parameter called Reynolds Number (Re). Reynolds Number is simply the ratio of internal resistance to viscous resistance over a flowing fluid. The Reynolds Number (Re) are formulated as:

$$Re = \frac{\rho D U_c}{\mu} \quad (1)$$

Where U_c is the velocity of the flow, D is the cylinder diameter, ρ is the density of fluid and μ is the dynamic viscosity of the fluid. As the Reynolds Number is increased, the flow begins to experience great changes.

Typical flow regime across pipeline illustrated in the Figure 2.5 below. The basis of formation of boundary layers of fluid around the pipeline can be explained as at very

low Reynolds number, the flow is smooth around the pipeline. But with the increase of the Reynolds number, boundary layers were detached from the sides of the pipeline. When $Re > 40$ due to adverse pressure gradient of the pipeline or cylinder surface, the boundary layer will be separated. As described in the Figure 2.5, inertia effects are almost negligible at a very low Reynolds number, $Re < 5$ and the pressure recovery at the end of the cylinder is almost complete. Vortex shedding does not occur because the flow is properly represented at these Re values. Hence at a very low Reynolds number the streamlines of the resulting flow is perfectly symmetrical but however as the Reynolds number, Re is increased the flow becomes asymmetric. But a pair of vortices is formed as the Reynolds number Re is increased. When the Re is to be increase even further, the vortices elongates until it breaks away and formed a staggered vortex and periodic wake.

The vortex is laminar flow up to the value of $Re = 150$ and then it becomes turbulent flow when Re values reaches 300. Approximately 50 diameters downstream of the pipeline, the vortex degenerates into a fully turbulent flow. Re values at range of 300 to 3×10^5 is called as subcritical range. For subcritical range, the vortex is in turbulent and occurs at a well-defined frequency. Meanwhile a laminar-turbulent transition occurs at a more downstream point of the pipeline.

At higher supercritical values of $Re > 3 \times 10^5$, the shedding of vortices becomes disorganized and boundary layer separation becomes turbulent on both sides of the pipeline or cylinder and the vortex shedding is reinstated. Between the stagnation point and the separation point, located the region of transition to turbulence. $Re > 10^6$ the flow regime boundary layer is completely turbulent on one side and partly laminar and also partly turbulent on the other side of the pipeline or cylinder.

Meanwhile at $Re > 10^7$ the value of drag coefficient appears to be independent of Re but there are insufficient experimental data available for this end of range. For higher Reynolds number, Re vortices will be disappearing because of the high rate of shear and then being replaced by a highly turbulent wake. Thus here nearly all drag were held responsible by pressure drag since there are increases in the value of drag coefficient, C_d .

$$Re = \frac{UD}{\nu}$$

$$Re = \frac{5 * 0.15}{1.55 \times 10^{-5}} = 50,000$$

$$Re = \frac{30 * 0.15}{1.55 \times 10^{-5}} = 300,000$$

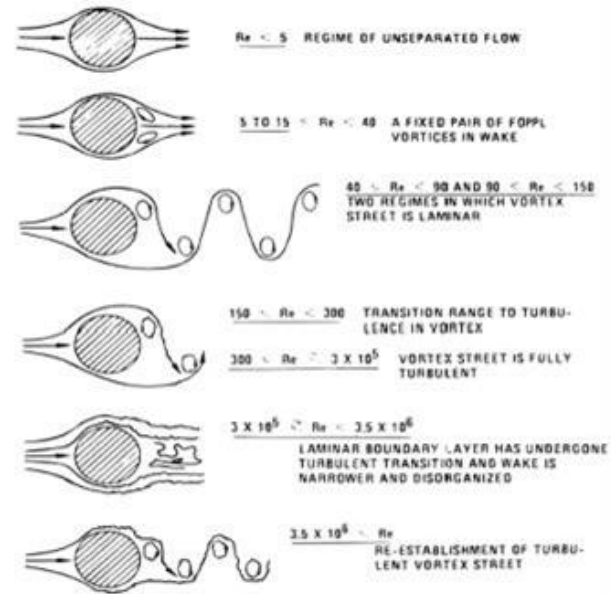


Figure 2.5: Cylinder Wake Pattern vs Reynolds Number (Wiggins, 2005)

The force component on the pipeline that been influenced by the cyclic change in the pressure distribution on the pipeline surface can be divided into two main parameter which are drag force which acts in the in-line of the flow direction and the lift force which correspond to the cross-flow direction. The drag also can be define as the component of the resultant force acting on the body when the body is in relative motion which is in the direction of it. Vortex induced vibration (VIV) are a major fluid load and fatigue component on pipeline. Fyrileiv et al. (2005) recorded a case of pipeline failure at East China Sea where Ping Hu pipeline failed at two locations in year 2000 due to VIV. This case is the most distinctive to show how vital VIV may affect pipelines. Therefore immediate measures must be taken seriously to suppress the shedding of the vortex streets. Reduction of vortex induced vibration (VIV) can be achieved by using VIV suppression device.

2.5 Drag

Drag force is a resistance or a force that acts opposite to an object that is moving in a motion through fluid. There are two classification of drag, when an object move in a motion through gas like air, it is called aerodynamic drag or air resistance. When an object move in a motion through liquid like water, it is then called hydrodynamic drag. Fluids are most certainly material but can either be liquid or gas. The principle property of material is to have both volume and mass. By mean to have a mass is that material tend to resist any changes in their velocity and by mean of having volume is that material tend to occupy space. The portion of the drag force is that is due to the resistance of the fluid to move or simply put, due to the inertia of the fluid is called the pressure drag.

A research on the drag amplification due to Vortex Induced Vibration was done by Griffin and Ramberg (). They used a theoretical formulation of drag force and reported a drag amplifications of cylinder oscillating due to VIV compared to stationary cylinders of around 2. Therefore, reduction of drag force experienced by the pipeline are very essential, because large drag forces may cause failure along the pipeline. The upward lift is contributed by the growth of vortex at lower edge of the pipeline or cylinder and meanwhile, the downward lift is contributed by the growth of vortex at the upper edge of the pipeline or cylinder. Both vortex gives an increase in the drag force. Total drag force of a pipeline is a combination of forces from both waves and currents, but in this research, the resultant drag force from current that only be taken into account.

Bernoulli's equation for the pressure in a fluid stated as:

$$P_1 + \rho g y_1 + \frac{1}{2} \rho v^2 = P_2 + \rho g y_2 + \frac{1}{2} \rho v^2 \quad (2)$$

Where in the first term of the equation is the part of equation that describes the inlet and outlet fluid pressure. The second term of the equation represent the gravitational contribution to the overall pressure. The third term is the dynamic contribution to the pressure or the kinetic to the pressure. To understand the origin of pressure drag, first need to solve for the equation of pressure as force per area.

$$P = \frac{F}{A} \equiv F = PA \quad (3)$$

Substitute the pressure in the equation above with the pressure in a moving fluid expression in the Bernoulli's equation.

$$F = PA = \left(\frac{1}{2}\rho v^2\right)A \quad (4)$$

Rearrange the equation in the term of drag force.

$$Fd = \frac{1}{2}\rho v^2 AC_d \quad (5)$$

Drag is majorly influenced by some other factors which includes shape, viscosity, compressibility, separation angle, boundary layer and lift. These factors can be piled into one monolithic fudge factor so called the coefficient of drag (C_d). Combining all these factors together yields a theoretically limited equation. The mean drag force, F_d of a pipeline in a current can be detailed as per equation:

$$Fd = \frac{1}{2}\rho U^2 A_f C_d \quad (6)$$

$$C_D = \frac{F_D}{\frac{1}{2}\rho U^2 DL} \quad (7)$$

Where ρ is the density, U is the velocity of fluid flows past the pipeline, A_f is the area of the pipeline (equal to length times diameter of the pipeline), and C_d is the coefficient of drag. It is noted that the coefficient of drag varies with Reynolds number.

2.6 VIV Suppression

In general there are two ways to reduce drag due to vortex induced vibrations (VIV) namely “active control and passive control”. The active control methods controls the flow by applying external energy by means such as the jet blow. Meanwhile, the passive control methods control the flow by altering the shape or geometry of the body or by attaching additives devices on the body. It is very clear that the passive method is much simpler and easier to realize compared to the active control which requires more complex machines devices which provide the external power to the flow consequently.

Some fruitful researches have been already performed in such a case. For example, some authors have added splitter plates (Kwon and Choi 1996) to control and regularize the flow around a circular cylinder. A lot of studies were done about passive control techniques and one of them was an approach by (Igarashi and Tsutsui), who successfully installed a trip-wire in the separate shearing layer of a cylinder for Reynolds Number (Re) of 42000. The mean drag force acting on the cylinder were reduced by 20 to 30% by adding the trip-wire, where the largest reduction of drag detected when the trip-wire were installed at the angle of 120° at the stagnation point.

In addition, there are also control techniques performed using secondary small cylinder (Mittal and Raghuvanshi 2001). There are also authors that achieved passive flow control by introducing a porous interface between solid body and the flow in order to reduce the intensity of the vorticity production of the boundary layer (Bruneau and Mortazavi 2001). In the summer of 2005, Department of Naval Architecture and Marine Engineering, University of Strathclyde, Glasgow had an idea on adapting a helical grooves onto a cylinder as a method to reduce drag and suppress VIV. In analysing and interpreting the results, it was surmised that the grooves reduces drag by a factor of 30% (Huang, 2006). (Munenra 2015) proves that the adapting a V-type grooves onto a cylinder reduce the drag coefficient from 1.37 to 0.9781 (by 28.4%) compared to smooth cylinder at the same Reynolds number of $Re = 20000$.

Meanwhile, modifying a U- grooved cylinder reduces drag coefficient by about 18.6%, compared with the smooth cylinder at the same Reynolds number. The reason behind it is mainly because the vortex formation region behind U-grooved cylinder is smaller than for the smooth cylinder (Lim & Lee 2003). Besides, Janardhanan (2014) stated that by adapting marine fairings onto a cylinder shall reduce the drag coefficient from 1.45 to 1.01 (by 30.3 %) compared to smooth cylinder at same Reynolds number of $Re = 10000$.

2.7 Dimple

Many flow phenomena are present when investigation over an external flows around bluff body were done including flows separation, formation of wake region, development of boundary layer and vortex shedding. “Drag crisis” occurs when the drag on a body drops significantly when investigated over a range of Reynolds

numbers. The drag crisis happens in different magnitude depending on the physical geometry of the body. Efforts have been placed to investigate the mechanism of drag reduction with lots of method. One of the methods are passive flow control, such that by modifying the surface geometry of the body will affect the drag value. Addition of surface roughness on a body to reduce the drag and to modify the flow characteristic of a cylinder were effectively used in modern research.

Modification of surface roughness was implemented in golf ball design after golf observer noticed that flow flight performance were much better by a scratched and dented golf balls. This findings had led to the dimpling technique used in manufacturing golf balls. The work presented explains a bit about how dimple can trigger drag reduction on a cylinder. A numerical study of the flow around dimples on a golf call done by Smith, C.E (2011) proves that a mechanism of drag reduction due to dimples. Measurement and study of flows over a golf ball have produced some understanding of mechanism of drag reduction by dimples. Some researcher measured the aerodynamic forces of spinning golf ball at Reynolds number of 94000 by noting the impact point after the call was dropped through the horizontal flow in a wind tunnel. Next major contribution were made by Bearman & Harvey (1993) as they measured the aerodynamic forces of a spinning golf ball over a range of Reynolds number. The most recent findings is from Choi et al (2006) who measured the gathered turbulent statistic of flow in order for him to understand the turbulence generation by dimples and how they trigger the reduction of drag on a golf ball.

From the literature study above, it is clear that initiation and progress had been made in understanding the fundamental mechanism of drag reduction of flow over dimpled surface. Therefore, in this present work, dimpled surface will be adapted on a concrete layer that normally coats a submarine pipeline and will be numerically simulated over a range of Reynolds number ($Re = 1 \times 10^4$ to 2.5×10^6)

CHAPTER 3: METHODOLOGY

A sequence or steps of the methodology have been set primarily to achieve the objective of this project. The methodology consists of two parts which are the overall project methodology and the numerical method simulation methodology.

3.1 Project Methodology

1. Identifying the problems.

- a) The problems need to be identified first in order to initiate the research. The accurateness for the problems chosen will improve accuracy on the direction of the research target rather than going on blindly. For this case, there are a few problems identified. The main problem is regarding the VIV formation for pipeline under free spanning condition.

2. Identifying the objectives and scope of study.

- a) In order to achieve the main target of this project, a very clear, concise and specific objectives need to be underline and the scope of study also need to be set in conjunction to be more specific on the research.
- b) In this very project, a sets of objectives and scope of study were identified. One of the objectives would be to analyse the effect of adapting the dimpled shaped concrete coated pipeline on VIV under free-spanning condition.

3. Gathering information

- a) Once the objectives have been set, the data gathering will be conducted as much information are needed before undergoing the simulation. The primary source of this research would probably come from reading material such as articles, journals, research papers, technical papers, conference papers and books.

- b) Meanwhile for data related to the key parameters such as pipeline data, concrete coatings data, sea scatter and other metocean data will be closely consulted by the engineers from the industry.

4. Ensuring the integrity of the data collected

- a) Data quality need to be assured first before proceeding to any design or simulation work. Therefore, all the data obtained need to be cross-checked with engineers from industry to ensure its reliability.

5. Designing and simulating the dimpled concrete coating pipeline

- a) Once the data is ensured reliable, the designing of dimpled pipeline coating will be done by using design software AutoCad or Catia. Then the design itself will be exported for the numerical simulation using Computational Fluid Dynamics software, specifically ANSYS Fluent.
- b) The simulation will be conducted using ANSYS Fluent and will simulate real condition of a free spanning pipeline under harsh sea condition with high number of waves and current. The outcome of the simulation shall be the predicted drag coefficient, value for drag force, and the separation angle.

6. Interpreting Data

- a) Once the simulation is done, the data collected from the simulation will be analysed and interpreted. This process is important to verify the output of the simulation.
- b) A close collaboration with the engineers from the industry also plays vital role during this stage of research as their views and thoughts may be as equally important in order to achieve the objectives of this research.

7. Conclusion and Recommendations

- a) Based on the outcome of the simulation, a meticulous conclusion shall be drawn to decide whether the output has met the objectives of this research.

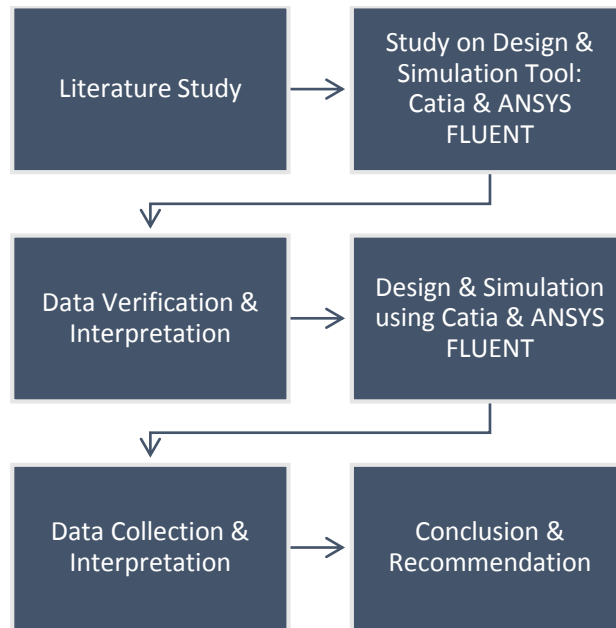


Figure 3.1: Overall Project Methodology

3.2 CFD Methodology

Computational Fluid Dynamics simulations processes could be categorized to three main phase. They are first pre-processor phase, then is solver or simulator phase and lastly is the post-processor phase. Pre -processing phase is the first stage where the geometry is being modelled and are defined as the fluid solution domain. During pre-processing phase also the design geometry (model) is meshed or turned into millions of discrete cells. Some key parameters need to be defined during this phase such as, the physical modelling, environmental behaviour and parameter, fluid domain properties and the model's boundary conditions. Moving on to the next phase is the simulator where the fluid flow equation is solved numerically by using numerical methods of either finite difference method (FDM), finite element method (FEM) or finite volume method (FVM). The post-processor phase shall be the last phase in CFD simulation process. The main output of the post-processing phase are to analyse the results and produce any visualization results available from the solution. A lot of CFD method able to produce a complete results with explicit data visualization. Here, data visualization consisting of the solution domain with grid display, contour plot of velocities and pressure, two-dimensional and three-dimensional vector plots and also particle tracking.

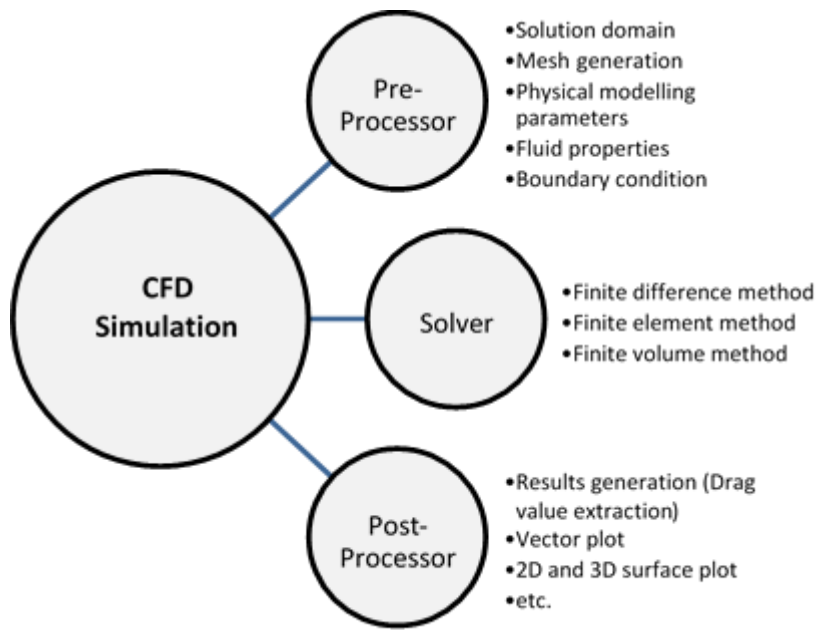


Figure 3.2: CFD Methodology

3.2.1 Fluid Solution Domain

The fluid solution domain could easily be define as the abstract territory where the equation of CFD solution is calculated and solved. The shape of the fluid territory can be either in circular or rectangular shaped. The chosen computational domain is a two-dimensional domain of a rectangular box shape as shown in Figure 3.2. Ong et al. (2008, 2010) used a two-dimensional fluid domain of (X, Y) 30D, 10D. Lei et al. (2000) used a two-dimensional fluid domain of (X, Y) 26D, 10D. The fluid domain is illustrated in Figure 3.3. With (X, Y) 28D, 11D.

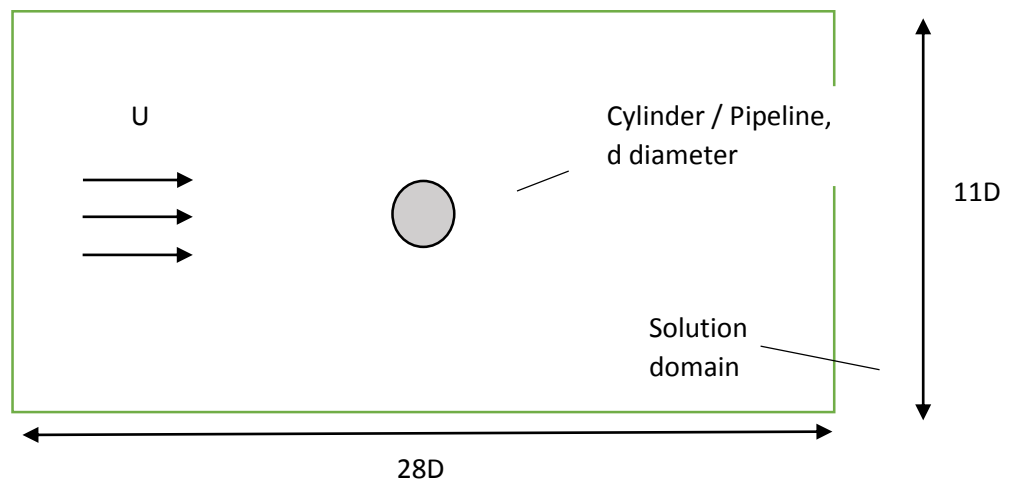


Figure 3.3: Rectangular Shaped Fluid Solution Domain (L x D)

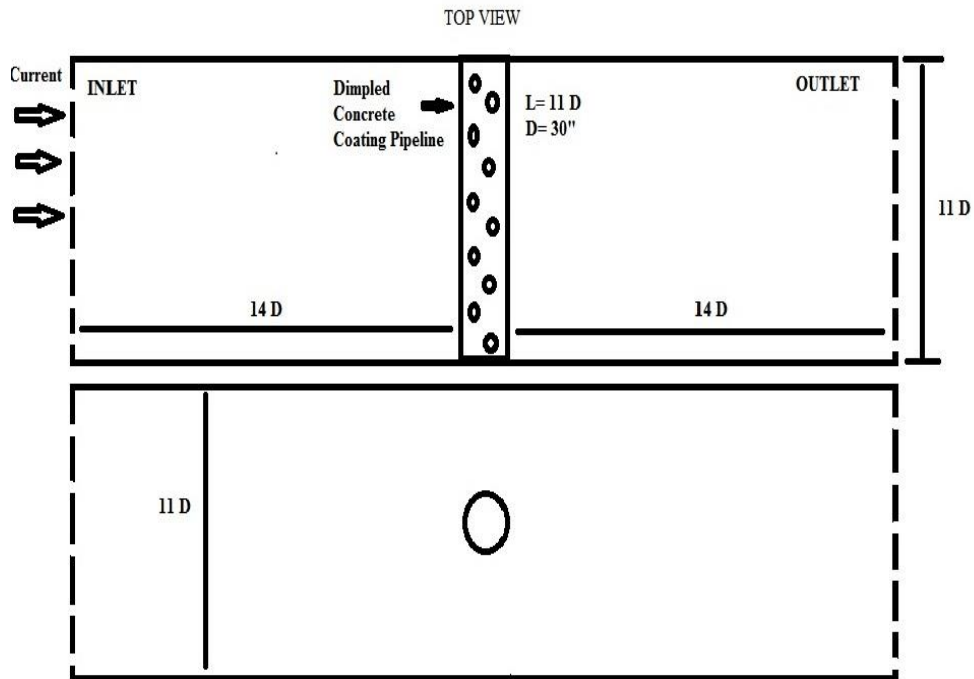


Figure 3.4: Top view of Fluid Domain

3.2.2 Modelling Geometries

Three different configurations are studied. They are (1) the normal or regular smooth surface pipeline, (2) pipeline adapted with dimple, $k/d = 3 \times 10^{-3}$, (3) pipeline adapted with dimple, $k/d = 4 \times 10^{-4}$ and Figure 3.5 shows all three different configurations being studied.

Both model of cases are made of concrete to match the actual application for subsea pipeline with the size of 30 inch (0.762 m) in diameter. In the present study, the dimples in the form of arc was used. And more, the depth ratio of the dimple to the pipeline diameter (k/d) (k : the depth of dimple) was 0.003018. The width ratio of dimple to pipeline diameter is constant value (c/d) (c : the diameter of dimple) at 0.08199. There was a total of dimples distributed over the two-dimensional pipeline. The gap between dimples are called pressure hole. There were pressure holes on the

dimpled pipeline surface which is 0.0151 m in size. Table 4.1 shows the key parameter of the pipeline geometry.

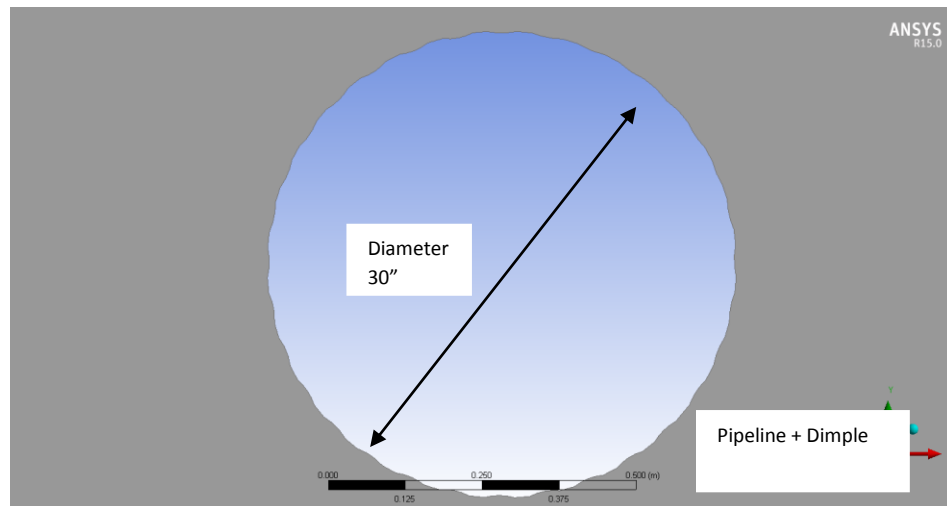


Figure 3.5 Geometry of dimple ($k/d = 3 \times 10^{-3}$)

3.2.3 Mesh Generation

After defining the fluid domain, then the mesh need to be generated within the fluid domain. In general, the mesh generation or grid generation is establish as the distinct locations at which the variables are ready to be calculated and to be solved by the simulator. The number of element in X and Y direction is based on the mesh convergence study. The mesh convergence study are further discussed in chapter. Shown in the Figure 3.6 is the structured mesh with the most optimum number of elements of 133 241 elements of the full fluid domain. 69 058 number of nodes were generated inside the fluid domain.

Inflation mesh are implemented within this structured mesh in order built a sufficiently fine mesh to adequate capture regions (the cylinder or pipeline) where flows will experience most important changes in key parameters such as velocity. Therefore, inflation layer meshing needed to be used to accurately capture the boundary layer region of the cylinder. There are 30 layers of inflation layer meshing used around the

cylinder with total thickness of 0.004 m. Figure 3.8 shows the inflation layer around the cylinder and Figure 3.9 shows a zoom-in inflation layer meshing.

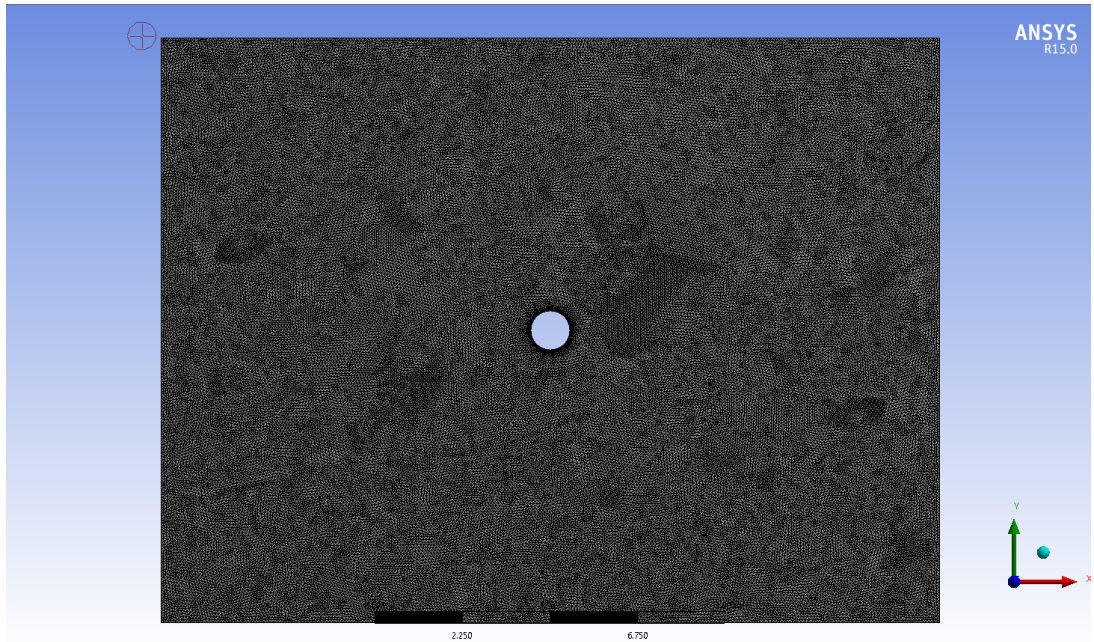


Figure 3.6: Structured Grid Mesh

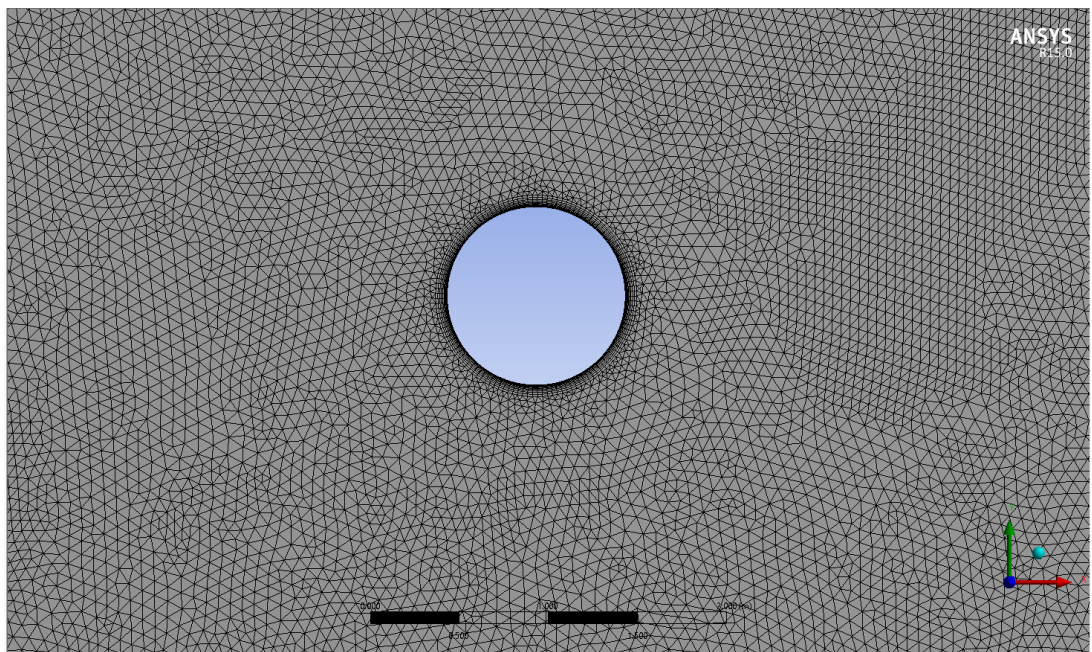


Figure 3.7: Inflation layer around cylinder

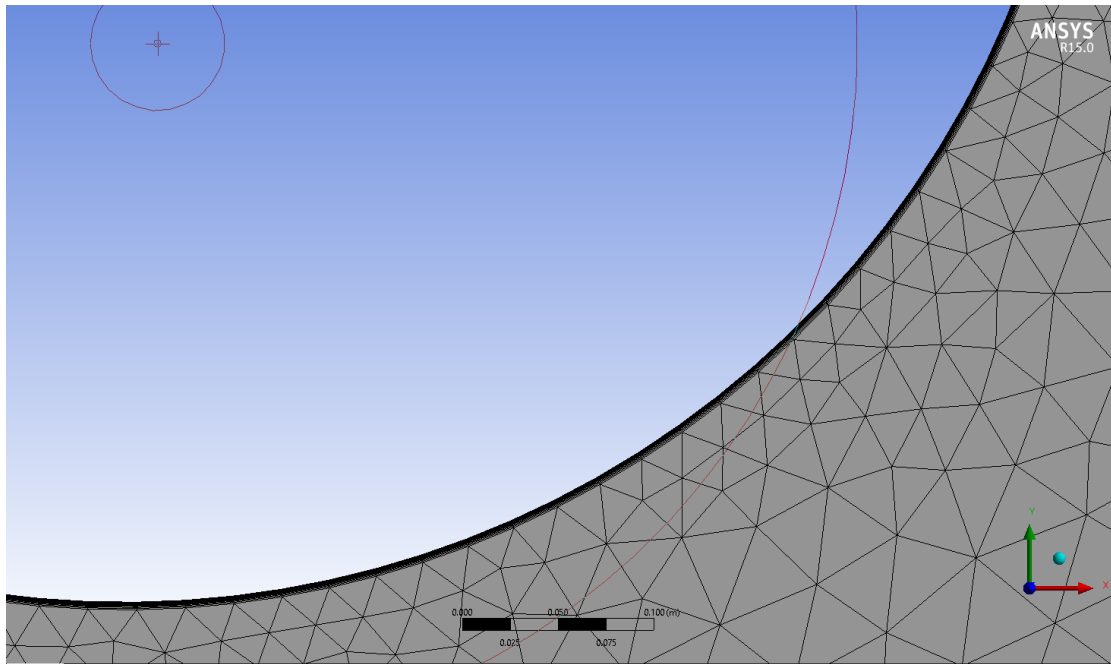


Figure 3.8: Zoom-in Inflation layer meshing around cylinder

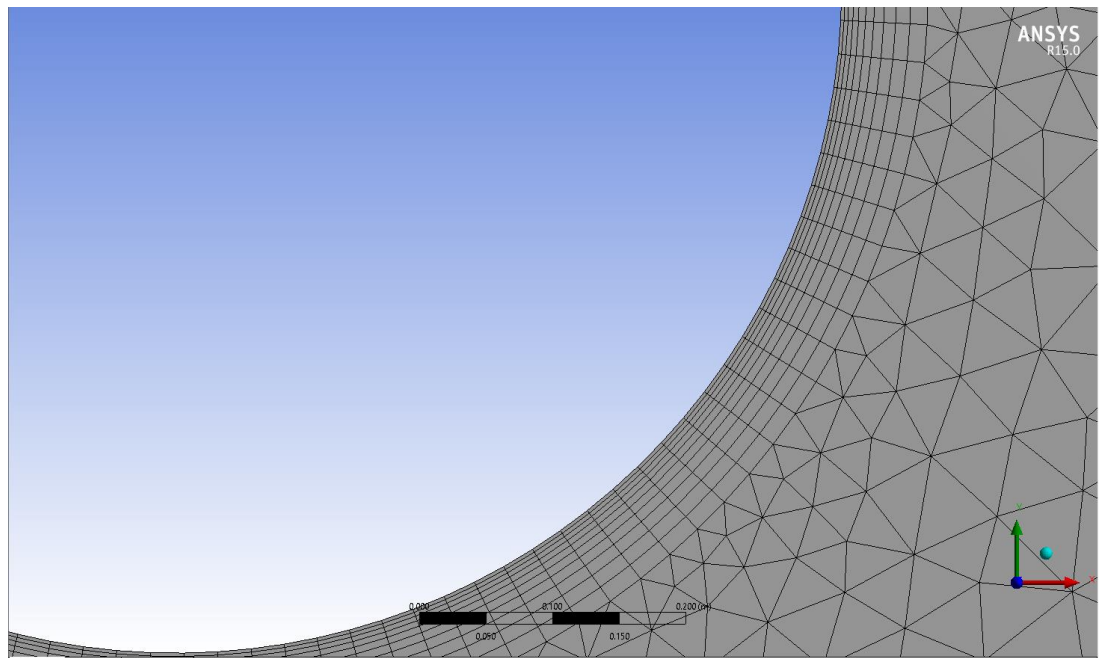


Figure 3.9: Zoom-in Inflation layer meshing around cylinder

3.2.4 Boundary Condition

a. Inlet Boundary Condition

The inlet boundary condition here allows the any type of flow parameter to enter the fluid solution domain. For this study, the inlet boundary condition will be set the velocity inlet. Details of this parameter is tabulated in Table...

b. Outlet Boundary Condition

The outlet boundary condition allows the flow parameter to exit the fluid solution domain and again for this study, the outlet boundary condition is set to be zero pressure.

c. Wall Boundary Condition

The wall boundary condition shall be defined for either laminar, transitional or turbulent flow. For this study, it will be defined as turbulent flow inside a pipe.

d. Periodic or Cyclic Boundary Condition

Periodic boundary condition is used when the model of the geometry and pattern of flow having a periodically or oscillatory repeating nature.

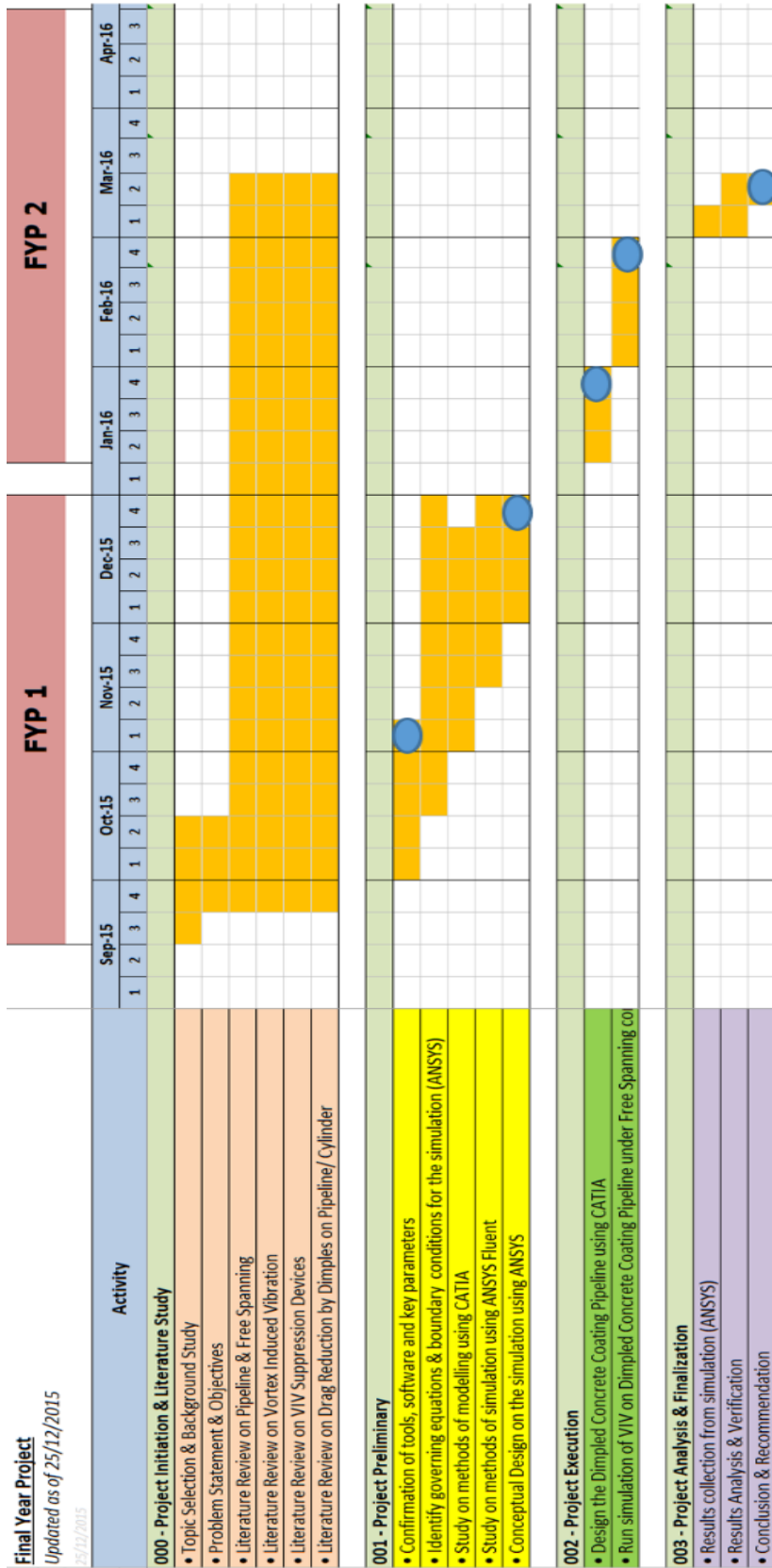
For this analysis, the initial condition was set for the inlet velocity, U_c of the uniform current at the inlet section. U_c was set for a range of 0.18 m/s to 1.8 m/s. The type of boundary conditions used are:

- Inlet section: Velocity Inlet. Uniform inlet velocity: $U_c = 0.18\text{m/s}$ to 1.8 m/s
- Outlet section: Pressure outlet
- Wall: Wall

Table 4.1: Summary of Main Parameter

	Case 1	Case 2	Case 3
Type	Smooth	Dimple	Dimple
Material	Concrete	Concrete	Concrete
Density (kg/m ³)	1025	1025	1025
Dimple depth (k/d)	-	3×10^{-3}	4×10^{-3}
Dimple width (c/d)	-	8×10^{-2}	6.5×10^{-2}
Inlet velocity (m/s)	0.18 – 1.80	0.18 – 1.80	0.18 – 1.80
Viscosity (kg/ms)	0.00096	0.00096	0.00096

3.3 Gantt Chart



CHAPTER 4: RESULTS AND DISCUSSION

Transient flow past a two-dimensional circular cylinder (pipeline) and a two dimensional dimpled shape cylinder are the point of interest in this study. In the present work, numerical simulation were performed by using ANSYS Fluent CFD code solving RANS (Reynolds Average Navier-Stokes) equation of Shear-Stress Transport SST $k-\omega$ model. Some cases with variant Reynolds number were simulated to investigate the drag and lift coefficient, flow separation angle, wake region size and pressure distribution on the body. The numerical results extracted having a good agreement with the experimental data from (Zdravkovich, 1997).

4.1 The Mesh Independency Study

The primary intention of conducting the mesh independency check is to justify the optimum size of the mesh in order to maintain the integrity and accurateness of the results produced. The mesh independency study is considered to be successfully attain when the output of the simulation is no longer being affected by the size of the mesh. Which means the results will maintain to be converge at same value regardless of any changes in grid size. A set of simulation were tested and it's comprised of a number of simulations of the 2- dimensional transient flow over cylinder at $Re = 40$. Simulation has been carried out for different size of grids. The main output of this simulation is the drag coefficient (C_d) and a summary of the simulations results is presented in Table 4.1.

Table 4.2: Summary results of Mesh Independency Study

Simulation Number	No of Element	Cd
S1	7143	1.4357
S2	7601	1.4384
S3	12599	1.4434
S4	68375	1.4510
S5	81325	1.4548
S6	102469	1.4560
S7	133241	1.4566
S8	178747	1.4576
S9	254363	1.4586

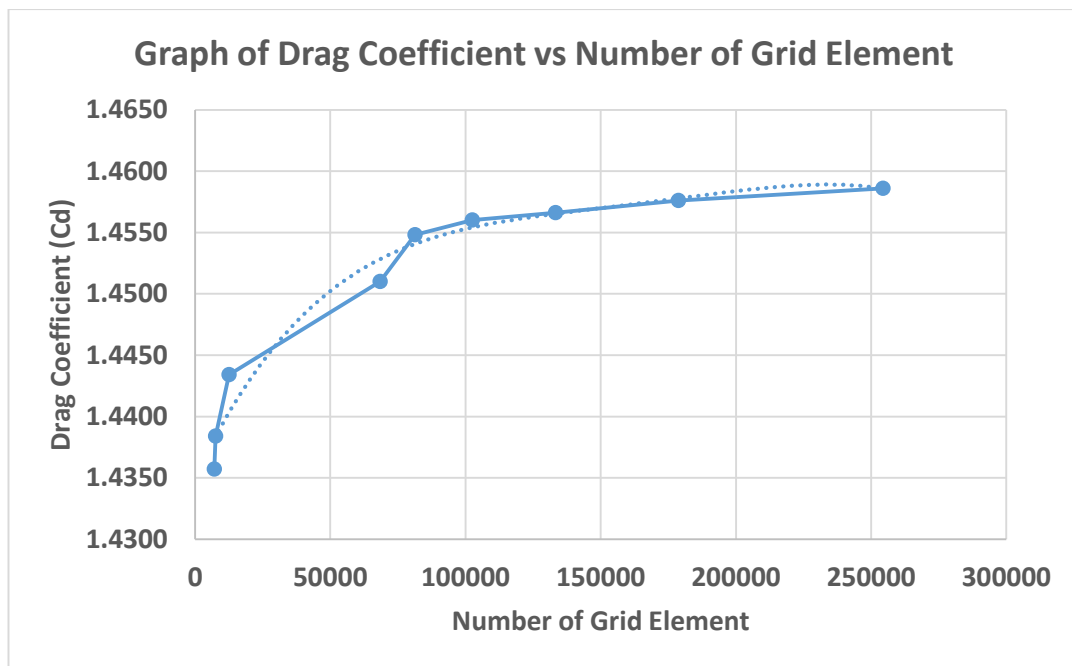


Figure 4.1: Graph of Drag Coefficient vs Number of Grid Element

The summary of Grid Convergence study are presented in which a solution functional in a graph of Drag Coefficient versus Number of Grid Element as the metric for the grid convergence verification. As illustrated in Figure 4.1, solution starts to reach asymptotic converge of the drag coefficient (Cd) at 6th simulation. Thus, the convergence here shows that the number of elements used within the mesh for all

Reynolds numbers are sufficiently resolved to approach the asymptotic range of solution.

It is an important to validate the accuracy of the method used. In order to validate the method used in this study, flows of differing Reynolds number were taken into account. Differing Reynolds number here by different its viscosity and free stream velocity. Some example are discussed herein. The first case is the simulation of the flow at $Re = 1 \times 10^5$. The flow was simulated and is visualized in the chapter 4.2

4.2 Flow Visualisation – Near Wall Region

Flow separation occurs when a point that the boundary layer travels far against an adverse pressure gradient that the ratio of relative speed of the object to the boundary layer so much lower as almost to zero. The flow being detached from the surface and transform to the form of vortices and eddies. Flow separation also can be define as the flow closest to the wall or leading edge reverse in direction. The separation point is defined as the point between the forward and reverse flow, where the shear stress is almost zero.

Both bare pipeline and dimple concrete coated pipeline were simulated for flow over a cylinder at a range of Reynolds number of $Re = 1 \times 10^4$ to 2.5×10^6 . A representative example of the simulation is the simulation at $Re = 1 \times 10^5$. Instantaneous contours of the flows characteristic and vorticity are illustrated in Figure 4.2. Surface of the instantaneous velocity magnitude were coloured by various contour of colour to exhibit the magnitude of velocity around the cylinder.

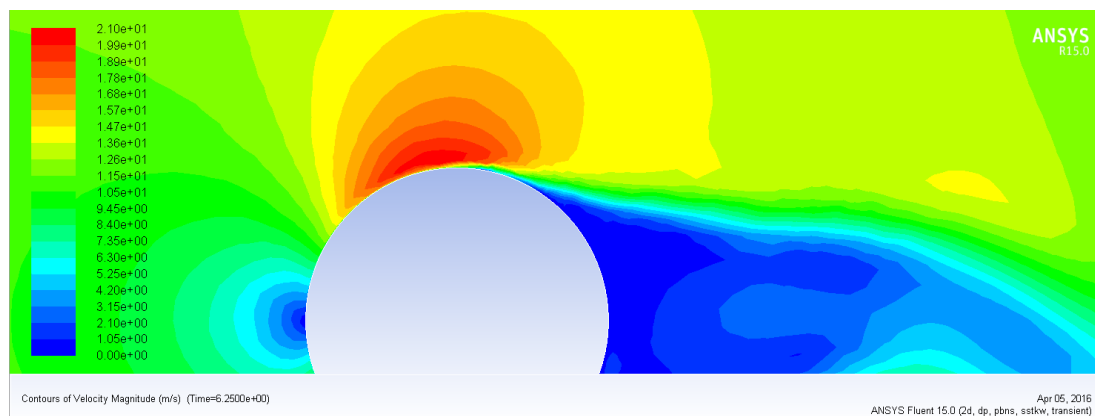


Figure 4.2: Instantaneous contours of the velocity, $Re = 1 \times 10^5$ for Case 1

Visualization of the instantaneous flow characteristic near wall region on bare pipeline (Case 1) can be seen in Figure 4.2. Simulation at Reynolds number of $Re = 1 \times 10^5$ for flow over bare pipeline shows a large flow separation in the wake region. Also observed that an early separation occurs that leads to the large amount of drag on the bare pipeline. For the Case 1, the separation point is at $\theta = 80^\circ$ and the separation point can be visualized in Figure 4.3.

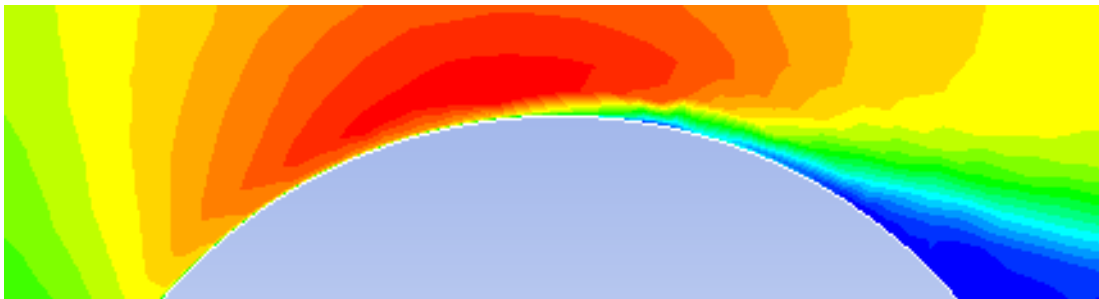


Figure 4.3: Instantaneous contours of velocity view at separation point, $\theta = 80^\circ$ for Case 1

On the other hand, visualization of the instantaneous flow characteristic near wall region on dimpled pipeline (Case 2) can be seen in Figure 4.4. Simulation for dimpled concrete coated pipeline at Reynolds number of $Re = 1 \times 10^5$ shows that the dimples causes separation to occur at much later in the downstream side of the flow creating a more narrow wake which leads to a less drag coefficient.

Dimples also can be seen changing the flow pattern to be turbulent even at a much lower Reynolds number. The separation point for dimpled concrete coated pipeline at Reynolds number $Re = 1 \times 10^5$ is at $\theta = 92^\circ$ as shown in Figure 4.5. Furthermore, as the depth of dimple becomes deeper (Case 3 & Case 4), the separation point shifts to a more upstream side of the pipeline as shown in Figure 4.6.

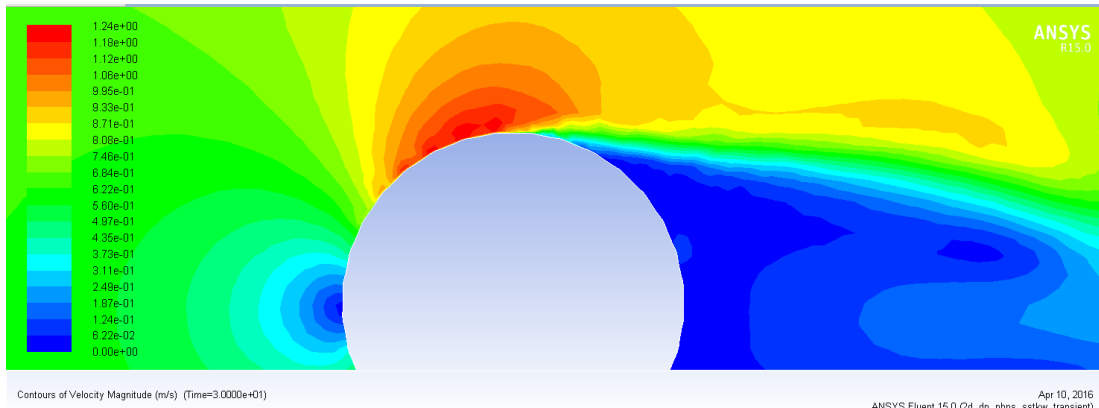


Figure 4.4: Instantaneous contours of the velocity, $Re = 1 \times 10^5$ for Case 2

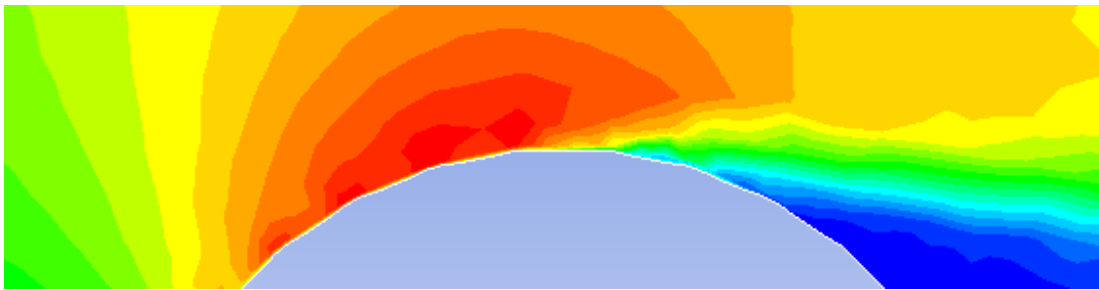
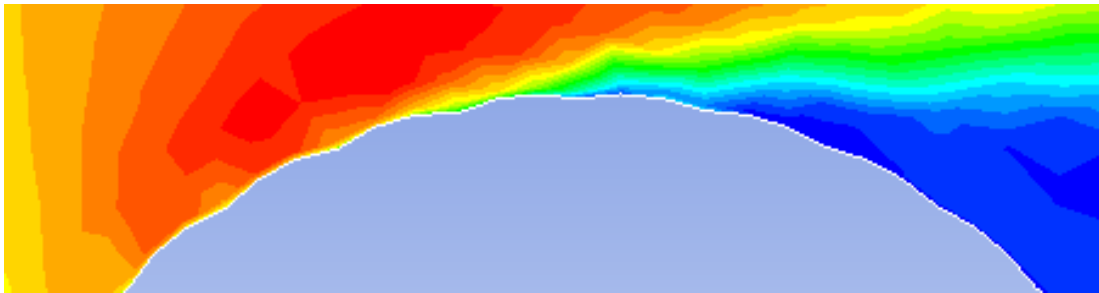
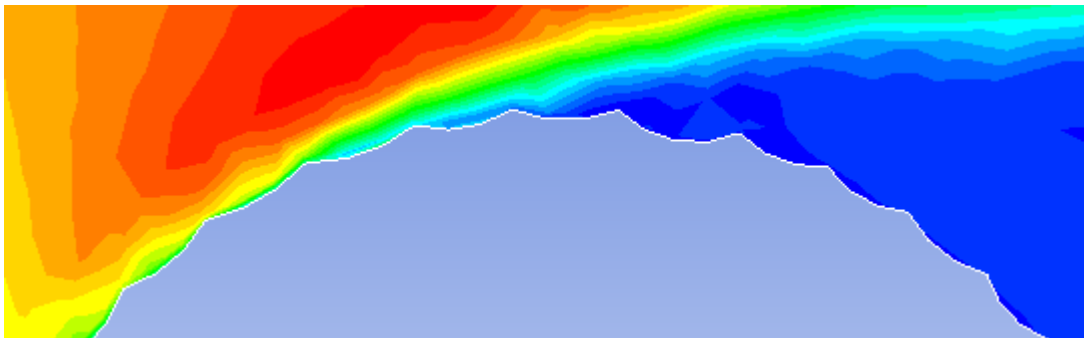


Figure 4.5: Instantaneous contours of velocity view at separation point, $\theta = 92^\circ$ for Case 2



(a)

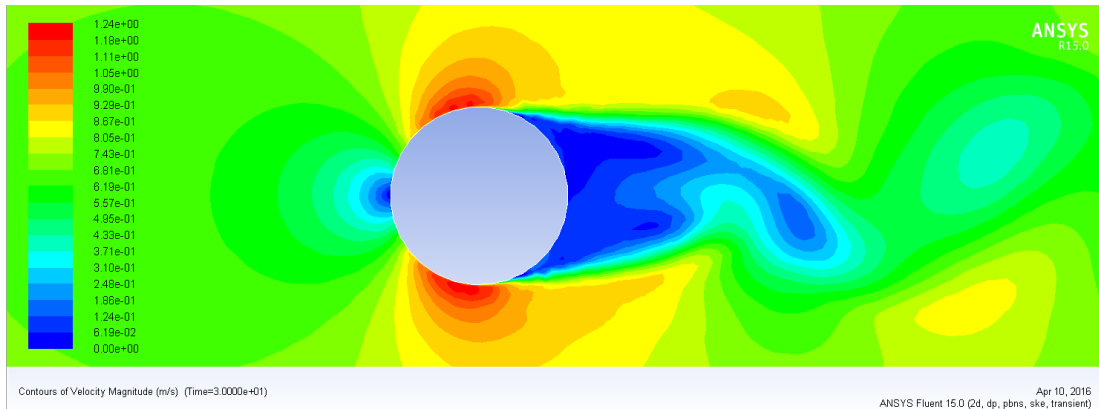


(b)

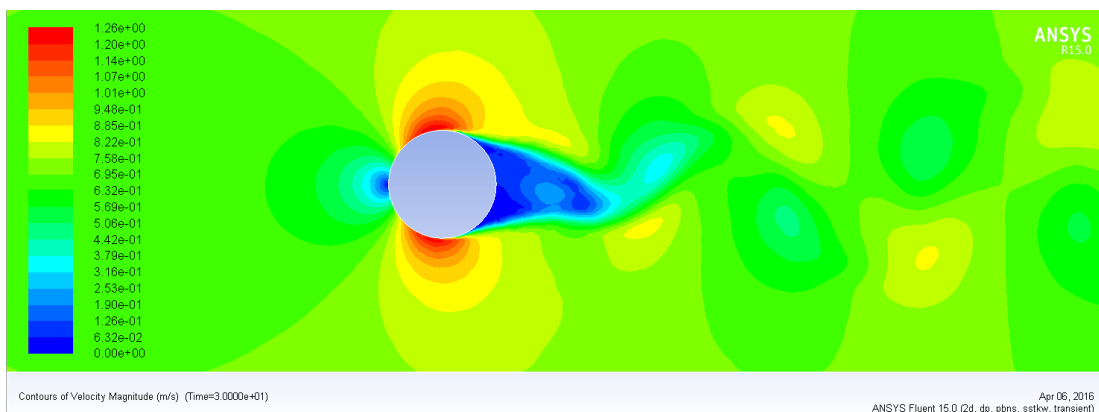
Figure 4.6: Instantaneous contours of velocity view at separation point (a) $\theta = 76^\circ$ for Case 3; (b) $\theta = 70^\circ$ for Case 4.

4.3 Flow Visualisation – Wake Region

As suggested by visualized results in the near wall region in Chapter 4.2, complete detachment happens at a point much earlier for Case 1 (bare pipeline) compared to Case 2 (dimpled pipeline), but on the other hand, the flow separation point occur at a more downstream side of the body for Case 3 ($k/d = 3 \times 10^{-3}$) and Case 4. Other validation cases was simulated for flow over a cylinder at a range of Reynolds number of $Re = 1 \times 10^4$ to 2.5×10^6 . A representative example of the simulation is the simulation at $Re = 1 \times 10^5$. Figure 4.7 illustrate the major differences between two cases in term of wake region. Case 2 shows the flow detachment which is shifted further into the downstream side of the body and shedding a vortices in a smaller wake region. Case 1 illustrate flow detachment at early point compared to Case 2 and also produces larger wake region.



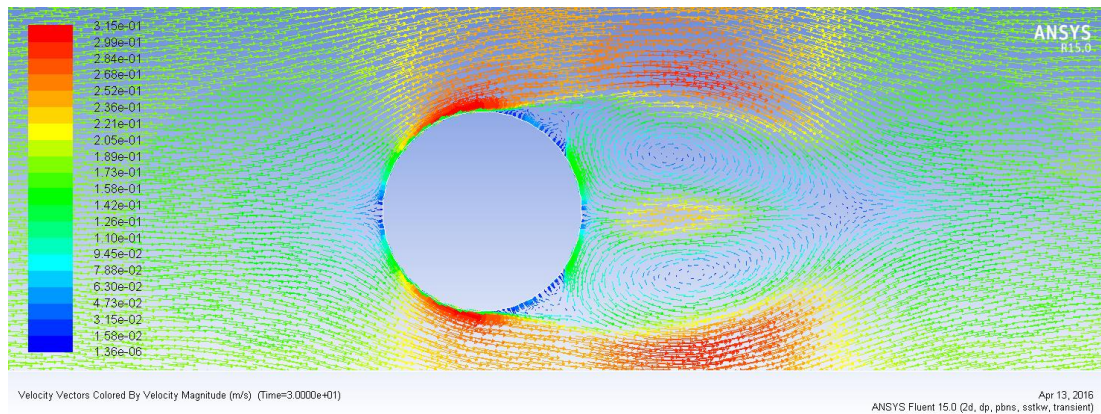
(a)



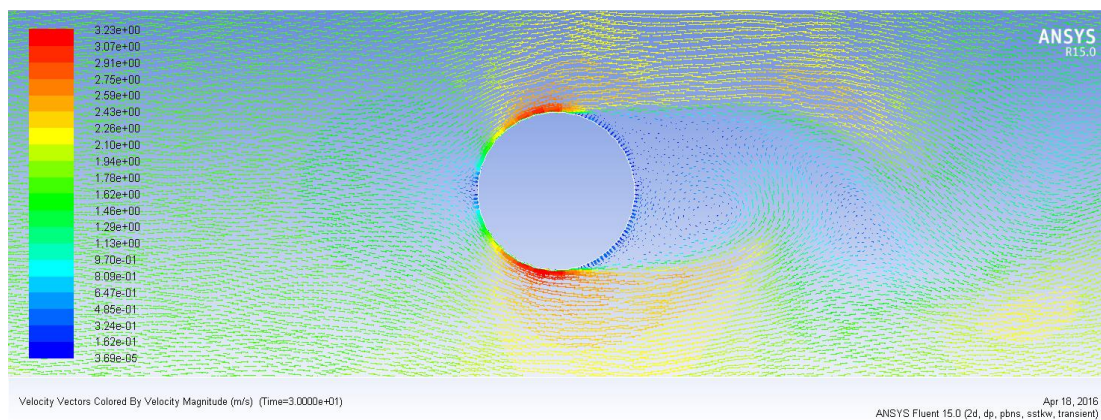
(b)

Figure 4.7: Instantaneous contours of vorticity (wake region) at $Re = 1 \times 10^5$, for (a) Case 1; (b) Case 2.

As we look deeper into the wake region size and the Von Karman Vortex Street for both Case 1 and Case 2, the generation of vortices within the dimple shed a much smaller vortices street compared to bare pipeline shed a larger magnitude of vortices. Figure 4.8 shows a new insight of recirculation flow zone behind the body. As the surface roughness increases, the re-circulation zone gains more strength and extends further towards downstream of the body. The vortices created for Case 2 cases a significant pressure and velocity gradient and then is where fluctuation take places as lift forces. This will be discuss more on Chapter 4.4.



(a)



(b)

Figure 4.8: Instantaneous velocity vectors for Case 2 at (a) $Re = 3 \times 10^5$;
(b) $Re = 4 \times 10^5$

4.4 Forces and Coefficient

The main parameter that play a vital role in the flow over a bluff body is the Reynolds number, as it dominantly determines the nature of the flow characteristic, boundary layer development, fluid forces and coefficient on the body, and wake region dynamics of the flow. Reynolds number is a non-dimensional value of the flow velocity of the fluid domain (U_c) on the density (ρ) and size of the body (D) by the dynamic viscosity of the fluid domain (μ).

$$Re = \frac{\rho D U_c}{\mu} \quad (1)$$

Drag crisis causing the drag coefficient on the bluff body to decrease dramatically at a critical Reynolds number. Achenbach (1972) stated that for a sphere, the drag crisis normally occurs around $Re = 400000$ (4×10^5). Therefore, as stated at earlier part of this report, in order to validate the methodology of this study, flows of differing Reynolds numbers were investigated as a base case.

Differentiating the Reynolds number was based on manipulating the freestream velocity at inlet of the fluid domain and based on the viscosity of the solution domain. Diameter of the bluff body (bare pipeline or dimpled concrete coated pipeline) of 0.762m and the density of the fluid domain (seawater) of 1025 kg/m^3 were set to be constant throughout the study.

The drag coefficient are bench-marked against published results of analysis and experiments. Figure 4.9 provides a comparison of drag coefficient from other scholar works that will be used for validating and bench-marking the results which will be extracted from the CFD simulation later.

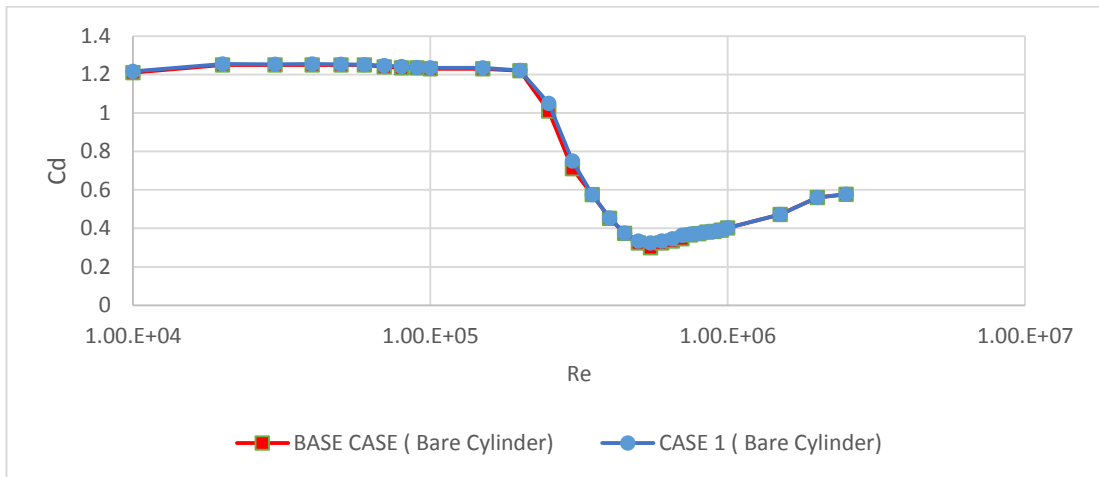


Figure 4.9: Variation of Cd with Reynolds number for smooth cylinder (Achenbach, 1972) and present result from Case 1

Critical Reynolds number regime starts at a point where the drag coefficient falls sharply for a bluff body placed in a velocity stream. Generally, for a cylinder with a smooth surface, the drag crisis occurs at a Reynolds number of around $Re = 300000$ (3×10^5). The adaptation of surface roughness on a surface at Reynolds number below this value can be very effective means of reducing the drag coefficient. However, as shown in the Figure 4.10, as the Reynolds number increase, the drag coefficient reduction of a dimpled pipeline through its critical Reynolds number regime is less than for bare pipeline at range of $Re = 4 \times 10^5$ to 2×10^6 .

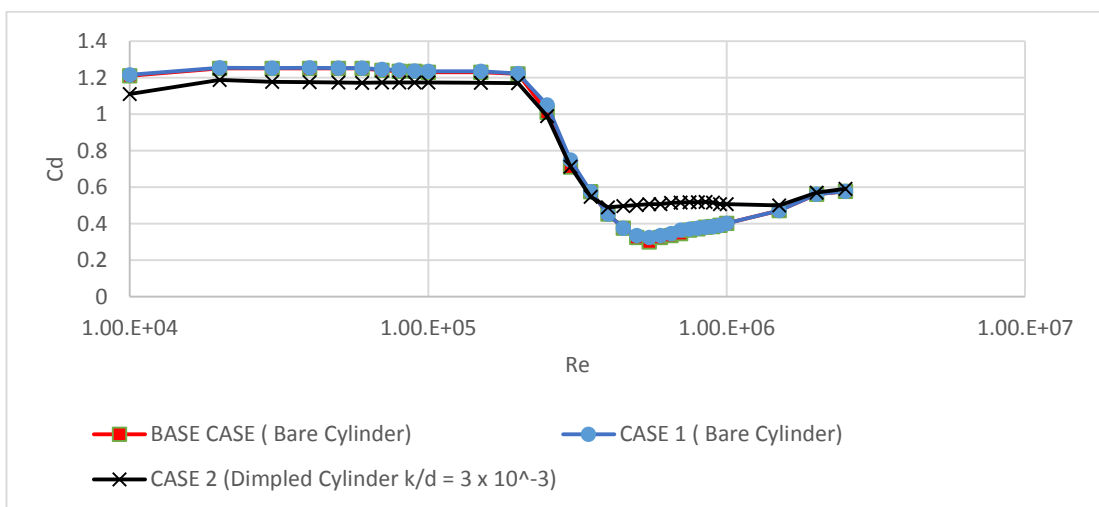


Figure 4.10: Graph of C_d vs Reynolds number for smooth cylinder (Achenbach, 1972) and present result from Case 1 and Case 2

In the present study, we have shown that a significant delays in point of separation from $\theta= 80^\circ$ to 92° , resulting in a drag reduction at $Re = 1 \times 10^4$ to 4×10^5 . This results from the generation of high momentum boundary layer within dimples and thus delay the separation through the shear layer instability. Furthermore, the variation of drag coefficient with Reynolds number from the base case being compared to Case 1 was nearly the same, so that we can conclude that this project having validated thoroughly by published work. Some previous studies strongly support the present mechanism of drag reduction by dimples. Finally, the present study suggest that for the application of dimple on a concrete layer coating of pipeline reduced drag at $Re=1 \times 10^4$ to 4×10^5 . It also suggest that the point of separation can be delayed up to $\theta= 92^\circ$ and producing a much smaller wake region and showing smaller eddies of vortices.

CHAPTER 5: CONCLUSION AND RECOMMENDATION

CFD method has been used to investigate the flow characteristic and exquisite detailed physics of flow over a normal bare pipeline or cylinder and has been used also to investigate the flow characteristic over a dimpled concrete coated pipeline in a range of Reynolds number from $Re = 1 \times 10^4$ to 2.5×10^6 . The numerical study were performed using the code ANSYS FLUENT by solving Reynolds Average Navier – Stokes (RANS) equations using k- ω SST model. The simulation were then used to simulate one case of bare pipeline and three cases of dimpled pipeline which involves in altering the geometry and size of the dimple. Detailed summaries of each cases are presented in Chapter 4 Result and Discussion. This chapter are majorly a condensed version of Chapter 4 which highlight the significant contribution of the research. Throughout this project, many interesting issues have arisen, which leads to some suggestions and recommendations for future direction of this project. Increasing surface roughness by using dimples may reduce VIV and could be an effective passive flow control. This project illustrate the connection between adapting dimples on a body and its effect on flow characteristic.

K- ω SST model has been used to investigate the effect of adapting dimpled concrete coated pipeline on the flow characterization in range of Reynolds number from $Re = 1 \times 10^4$ to 2.5×10^6 . Spanning the transition between the subcritical and post critical Reynolds number regime, there is a wide range of Re where the flow around circular body can be influence remarkably by increasing surface roughness of the body. For instance adapting dimple on a surface is one way of increasing the surface roughness.

Theoretically, the characteristic of flow over dimples on a pipeline is shown by development of vortices that originate from instabilities in the locally-detached shear layer. The flow boundary layer structure (turbulent) were form at location near the downstream side of the dimples and generate high momentum which overcomes the adverse pressure gradient. It also often with increased turbulence producing local flow reattachment near downstream of dimples.

In the present study, we have shown that a significant delays in point of separation from $\theta= 80^\circ$ to 92° , resulting in a drag reduction at $Re = 1 \times 10^4$ to 4×10^5 . This results from the generation of high momentum boundary layer within dimples and thus delay the separation through the shear layer instability. Furthermore, the variation of drag coefficient with Reynolds number from the base case being compared to Case 1 was nearly the same, so that we can conclude that this project having validated thoroughly by published work. Some previous studies strongly support the present mechanism of drag reduction by dimples. Finally, the present study suggest that for the application of dimple on a concrete layer coating of pipeline reduced drag at $Re=1 \times 10^4$ to 4×10^5 . It also suggest that the point of separation can be delayed up to $\theta= 92^\circ$ and producing a much smaller wake region and showing smaller eddies of vortices.

In conclusion, this study on drag reduction measure on dimpled concrete coating pipeline as a VIV suppression device can benefits the industry whereby it will help in mitigating VIV and thus avoid pipeline failure due to fatigue from excessive cyclic loadings. The project is within the capability to be executed by a final year student with the kind help and guidance from the Supervisor, Co-Supervisor and the course Coordinator. The time frame is also feasible and the project is expected to complete within allocated time. Recommendation that could be consider for future study is to include or take into account more parameters such as extensive metocean data and pipe-to-soil interaction. Another possible extension of this project may be to go for a three-dimensional modelling of the dimpled pipeline

CHAPTER 6: REFERENCES

- [1] Choi J, Jeon WP, Choia H. “Mechanism of Drag Reduction by Dimples on a Sphere.” *Physics of Fluids*. Vol.18 4 041702. (2006)
- [2] Jeon S, Choi J, Jeon WP , Choi H, Park J, “Active control of flow over a sphere at a sub-critical Reynolds number,” *J. Fluid Mech*. 517, 113 (2004).
- [3] Berthelsen, P.A. and Faltinsen, O.M. 2007. A local directional ghost cell approach for incompressible viscous flow problems with irregular boundaries. *Journal of Computational Physic* 227 (2008) 4354 – 4397.
- [4] Calhoun, D. 2002. A Cartesian grid method for solving the two-dimensional streamfunction-vorticity equations in irregular regions. *Journal of Computational Physic*. 176 (2) 231–275.
- [5] Janardhanan, A., "Reducing Vortex-Induced Vibration of Drilling Risers with Marine Fairing" (2014). University of New Orleans
- [6] P. W. Bearman and J. K. Harvey, “Golf ball aerodynamics,” *Aeronaut. Q.* 27, 112. (1976)".
- [7] Choi J, Jeon P.W, Choi H, “Mechanism of drag reduction by dimples on a sphere” (2006). School of Mechanical and Aerospace Engineering, Seoul National University
- [8] Bakhtiary, A.Y., Ghaheri, A. and Valipour, R. “Analysis of offshore pipeline allowable free span length,” *International Journal of Civil Engineering* 5-1 (2007)

- [9] Herfjord, K. 1996. A study of two-dimensional separated flow by a combination of the finite element method and Navier–Stokes equations. Dr. Ing.-Thesis, Norwegian Institute of Technology, Department of Marine Hydrodynamics. Trondheim, Norway.
- [10] Mehdi, Y., and Jabbari, E. “Determining natural frequency of free spanning offshore pipelines by considering seabed soil characteristics,” *Journal of Persian Gulf* 3-8 (2012)
- [11] Linnick, M. N and Fasel, H.F. 2005. A high-order immersed interface method for simulating unsteady compressible flows on irregular domains. *J. Comput. Phys.* 204 (1) 157–192.
- [12] Rajani, B.N. et al. 2008. Numerical Simulation of Laminar Flow Past a Circular Cylinder. *Journal of Applied Mathematical Modelling* 33 (2009) 1228-1247. Elsevier
- [13] Russel, D. and Wang, Z.J. 2003. A Cartesian grid method for modeling multiple moving objects in 2D incompressible viscous flow. *Journal of Computational Physic.* 191 (1) 177–205.
- [14] Fyrileiv, O., Chezhian, M., Soreide, T., Nielsen, F.G., and Mork, K. “Assessment of VIV induced fatigue in long free spanning pipelines”. 22nd International Conference on Offshore Mechanics & Arctic Engineering (OMAE), Cancun, Mexico. (2003)
- [15] Farrell, D.E., Hover, F., and Triantafyllou, M., “Vortex Induced Vibration of Cylinders: Experiments in Reducing Drag Force and Amplitude of Motion” (2007). United States Naval Academy and Massachusetts Institute of Technology
- [16] Taggart, S., Tognarelli, M.A., “Offshore Drilling Riser Supression Devices – What’s Available to Operators?” 27th International Conference on Offshore Mechanics & Arctic Engineering (OMAE), Estoril, Portugal. (2008)
- [17] Owen, J.C., Bearman, P.W., Szewczyk, A.A., “Passive Control of VIV with Drag Reduction” (2000)

- [18] Petrusma, M.S & Gai, S.L., “The effect of geometry on the base pressure recovery of the segmented blunt trailing edges” *Aeronautical Journal* 98, 267-274 (1994)